

Impact of new permittivity measurements on sea surface emissivity modeling in microwaves

C. Guillou,¹ W. Ellison,² L. Eymard,¹ K. Lamkaouchi,³ C. Prigent,⁴
G. Delbos,² G. Balana,² and S. A. Boukabara¹

Abstract. As part of a measuring program dedicated to the analysis of the dielectric properties of seawater in the frequency range 3–89 GHz, a new dielectric permittivity model based on the standard Debye theory has been developed for remote sensing applications over the ocean below 40 GHz, together with polynomial interpolations at the millimeter frequencies 85.5 and 89 GHz. The aim of this paper is to test the relevance of these new dielectric measurements through statistical comparisons of radiative transfer predictions with satellite and airborne radiometric data between 18 and 89 GHz. A radiometric sensitivity analysis to the permittivity measurement errors is proposed, which yields a sea surface brightness temperature accuracy of at least 0.5 K below 20 GHz, 1 K at 24 GHz, and 1.5 K at 37 and 89 GHz. At frequencies less than 40 GHz, superiority of the revised Debye model is pointed out over the most commonly used model of *Klein and Swift* [1977]. At millimeter frequencies the new permittivity expressions deviate significantly from the standard Debye predictions, especially at low temperature, suggesting the influence of a second “high-frequency” Debye relaxation. Our comparisons with radiometric data at 89 GHz and in the channel 85.5V of the special sensor microwave imager tend to support this hypothesis. The results emphasize the importance of an adequate modeling of the complex permittivity of seawater as input to the surface emissivity models, at any frequency of the microwave spectrum, and augur interesting outputs in both in-flight calibration and interpretation of satellite data.

1. Introduction

Recent advances in microwave technology now make possible the design of satellite operable radiometers at millimeter frequencies with sensitivities better than 1 K. The multifrequency imaging microwave radiometer (MIMR) with 12 channels between 6 and 89 GHz is one example. This instrument was designed by the European Space Agency (ESA) to observe the ocean surface for retrieving sea surface temperature and wind speed, as well as atmospheric quantities, from the future European Polar Platform. For remote sensing applications over the ocean a precise knowledge of the emissivity and scattering properties of the sea surface is required, as a function

of various instrumental and geophysical parameters (frequency and geometry of observation, sea state, salinity, water temperature, wind speed and direction, fetch, etc.). Physical approaches have been developed to predict the interaction of the sea surface with microwave radiation. Most of the available models focused on the problem of the surface roughness effects and more or less neglected the sensitivity to the seawater permittivity. When using physical approaches to simulate the passive microwave ocean signature, whatever the model, any uncertainty in the value of the permittivity has direct and important repercussions in the retrieved geophysical parameters [*Shutko et al.*, 1982].

In the early 1950s, several experiments were performed to measure the dielectric permittivities of aqueous ionic solutions as a function of temperature and concentration at various frequencies, up to 48.6 GHz [*Hasted et al.*, 1948; *Hasted and El Sabeh*, 1953; *Saxton and Lane*, 1952]. The first investigations concerning seawater samples were provided by the measurements of *Ho and Hall* [1973] and *Ho et al.* [1974] at very low frequency, below 3 GHz. Since 1974, there has been no comprehensive study for seawater or any

¹ Centre d'étude des Environnements Terrestre et Planétaires, Centre Universitaire, Vélizy, France.

² Laboratoire de Physique des Interactions Onde-Matière, ENSCPB, Université Bordeaux, Talence, France.

³ Département de Physique, Faculté des Sciences, Meknès, Morocco.

⁴ Goddard Institute for Space Studies, New York.

aqueous ionic solution for variable concentration, temperature, and frequency. In spite of the relative inaccuracy of experimental data, numerous authors have attempted spectral analyses under more or less plausible hypotheses [Stogryn, 1971; Wisler and Hollinger, 1977; Klein and Swift, 1977]. The standard assumption is that the permittivity of an aqueous solution, for a fixed temperature, follows a single Debye relaxation law over the frequency range 0–100 GHz. This common assumption is subject to caution today. Indeed, from recent very precise measurements for pure water, some authors note a departure from the simple Debye approximation below 100 GHz, especially at low temperatures. This discrepancy can be accounted for by invoking the existence of a second relaxation process [Grant *et al.*, 1981; Barthel *et al.*, 1991; Richards and Sheppard, 1991].

From the literature analysis a need was recognized for permittivity measurements of seawater in the frequency range 5–100 GHz, at temperatures and salinities representative of the world's oceans. In the context of MIMR preparation, such measurements have been conducted under well-controlled environment at 6.8, 10.65, 18.7, 23.8, 36.5, and 89 GHz [Ellison *et al.*, 1996a, this issue]. In this paper we present a brief description of the experiment and of the principal results. A comparison with the available literature is given in section 3. Finally, a radiometric sensitivity analysis to permittivity measurement errors is proposed in section 4, together with a discussion of the relevance of the new models compared with airborne and satellite radiometric data between 18 and 89 GHz.

2. Experimental Results

Conductivity and complex permittivity measurements of seawater, NaCl, and aqueous ionic solutions have been performed at the Laboratoire de Physique des Interactions Onde-Matière (PIOM) in France. The objectives of this program were to elucidate the role of organic matter and ionic content in the conductivity and permittivity of seawater and to provide a reliable interpolation model, as a function of frequency, temperature, and salinity for use in radiative transfer models up to 100 GHz. In this section we limit to the general outlines our description of the experimental procedure. Technical details are given by Ellison *et al.* [1996a, this issue].

Seawater samples were collected from different regions to cover the natural salinity variations over

the globe. Mediterranean Sea samples provided salinities at 38 and 38.9‰. Medium-salinity samples (35.7‰) were found in the mid-North Atlantic, while low-salinity samples were taken from the Atlantic-Gironde estuary, rich in sediment content (23.2, 28‰), and from polar seas (30.2‰). The measurements were performed between -2° and 30°C with two vector network analysers. Below 20 GHz, a Hewlett Packard 8510B analyzer was used to measure the transmission coefficient with a coaxial waveguide method. At frequencies 23.8, 36.5, and 89 GHz, an ABmm MVNA 8350 vector network analyzer was adopted, operating in a free-air propagation and transmission mode through a variable-thickness measuring cell. A temperature control system permitted having the complete range of temperatures (in 1° steps with the HP analyzer and at -2° , 12° , 20° , and 30°C with the ABmm system) stabilized to $\pm 0.01^{\circ}\text{C}$.

The permittivity measurements of seawater have been conducted with a precision of 1% at 6.8, 10.65, and 18.7 GHz and of 3% at 23.8, 36.5, and 89 GHz. Interpolation formulae for the real and imaginary parts of the complex permittivity ($\epsilon = \epsilon' - j\epsilon''$) have been derived as a function of the temperature (T) and the salinity (S) for each specific MIMR channel [Ellison *et al.*, 1996a]. The conductivity (σ) of the different seawater samples was measured as a function of the temperature by using a conductance meter. A polynomial regression fit to the data provided the following expression:

$$\begin{aligned} \sigma(T, S) &= d_1(T) + Sd_2(T) \\ d_1(T) &= 0.08637 + 0.03067T - 4.121 \times 10^{-4}T^2 \quad (1) \\ d_2(T) &= 0.07745 + 1.687 \times 10^{-3}T + 1.937 \times 10^{-5}T^2 \end{aligned}$$

The average difference between the interpolation formula and the measurements is less than 1%, which is perfectly adequate for any permittivity spectral analysis. Seawater is an aqueous multi-ionic solution, whose principal ionic constituent is NaCl. A natural question arose concerning a potential difference between the dielectric properties of seawater and NaCl, which was not clearly answered in the literature survey. Conductivity and permittivity measurements of seawater samples, NaCl solutions, and solutions consisting of a mixture of electrolytes (like in seawater) were thus compared. The results indicate that for the same salinity, NaCl has a conductivity higher by 3% than the natural and synthetic seawater. Given a same conductivity, however, the resulting permittivity

is the same, within the error bar of the measurements, for the different aqueous solutions. The organic content of seawater was also shown to have no measurable effect on its permittivity at any of the MIMR frequencies.

Since we are more widely interested in having the complex permittivity at any frequency, a spectral analysis of the data was carried out. It is generally accepted that for a fixed temperature in the frequency range 0–40 GHz, the dielectric behavior of pure water is very closely represented by a simple Debye relaxation [Ellison *et al.*, 1996b]. We supposed that in this frequency range an aqueous saline solution can also be adequately represented by a Debye relaxation together with a correction term for the ionic conductivity:

$$\epsilon = \epsilon_s + \frac{\epsilon_s - \epsilon_\infty}{1 + j2\pi\nu\tau} - j \frac{\sigma}{2\pi\nu\epsilon_0} \quad (2)$$

where ϵ_s and ϵ_∞ are the static and high-frequency dielectric constants, respectively; τ is the relaxation time in seconds; ϵ_0 is the permittivity of free space ($\epsilon_0 = 8.854 \times 10^{-12}$ F/m); ν is the electromagnetic frequency in Hertz; and σ is the ionic conductivity in mhos/m.

The Debye parameters τ , ϵ_s , and ϵ_∞ have been calculated using additional Hewlett Packard measurements for 201 frequencies between 3 and 20 GHz and for each sea sample at 1°C intervals in the range –2°–30°C. Polynomial interpolations have been deduced as functions of T and S . For a fixed temperature, τ (hereinafter equation (5) is given in picoseconds) and ϵ_s are linear functions of the salinity:

$$\epsilon_s(T, S) = a_1(T) - Sa_2(T) \quad (3)$$

in which

$$\begin{aligned} a_1(T) &= 81.82 - 6.050 \times 10^{-2}T - 3.166 \times 10^{-2}T^2 \\ &+ 3.109 \times 10^{-3}T^3 - 1.179 \times 10^{-4}T^4 \\ &+ 1.483 \times 10^{-6}T^5 \end{aligned}$$

$$\begin{aligned} a_2(T) &= 0.1254 + 9.403 \times 10^{-3}T - 9.555 \times 10^{-4}T^2 \\ &+ 9.088 \times 10^{-5}T^3 - 3.601 \times 10^{-6}T^4 \\ &+ 4.713 \times 10^{-8}T^5 \end{aligned}$$

$$\epsilon_\infty(T, S) = b_1(T) \quad (4)$$

in which

$$\begin{aligned} b_1(T) &= 6.458 - 4.203 \times 10^{-2}T - 6.588 \times 10^{-3}T^2 \\ &+ 6.492 \times 10^{-4}T^3 - 1.2328 \times 10^{-5}T^4 \\ &+ 5.043 \times 10^{-8}T^5 \end{aligned}$$

$$\tau(T, S) = c_1(T) + Sc_2(T) \quad (5)$$

in which

$$\begin{aligned} c_1(T) &= 17.303 - 0.6665 \times T + 5.148 \times 10^{-3}T^2 \\ &+ 1.214 \times 10^{-3}T^3 - 5.032 \times 10^{-5}T^4 \\ &+ 5.827 \times 10^{-7}T^5 \end{aligned}$$

$$\begin{aligned} c_2(T) &= -6.272 \times 10^{-3} + 2.357 \times 10^{-4}T \\ &+ 5.075 \times 10^{-4}T^2 - 6.398 \times 10^{-5}T^3 \\ &+ 2.463 \times 10^{-6}T^4 - 3.066 \times 10^{-8}T^5 \end{aligned}$$

The difference between the model predictions and the fits to the permittivity measurements does not exceed the experimental uncertainty at MIMR frequencies up to 23.8 GHz. At 36.5 GHz the comparison gives a fair but not perfect agreement, within 3%. This is interpreted as a limit of validity for the frequency extrapolation. The standard Debye equation (2), by means of (1), (3), (4), and (5), can be used to compute the complex permittivity of any natural seawater for $-2^\circ\text{C} \leq T \leq 30^\circ\text{C}$ and $20\% \leq S \leq 40\%$ in the frequency range 3–37 GHz with a maximum error of 3%, but certainly not higher. At 89 GHz, there is a total disagreement between the model predictions and the experimental values, especially at low temperatures. Therefore, for applications at 89 GHz, the regression fits based on the measurements at this specific frequency should be used to calculate ϵ' and ϵ'' . They are found to be independent of the salinity for the samples under consideration, within the 3% error estimate:

$$\begin{aligned} \epsilon' &= 6.963 + 4.937 \times 10^{-2}T + 3.855 \times 10^{-3}T^2 \\ &- 9.091 \times 10^{-5}T^3 \end{aligned} \quad (6a)$$

$$\begin{aligned} \epsilon'' &= 9.971 + 1.971 \times 10^{-1}T - 8.274 \times 10^{-4}T^2 \\ &+ 6.400 \times 10^{-6}T^3 \end{aligned} \quad (6b)$$

To assess this cubic interpolation polynomial, additional data for an aqueous NaCl solution (35%) were used, with a narrow temperature sampling (1° steps from 0°C to 25°C). Further high-frequency measure-

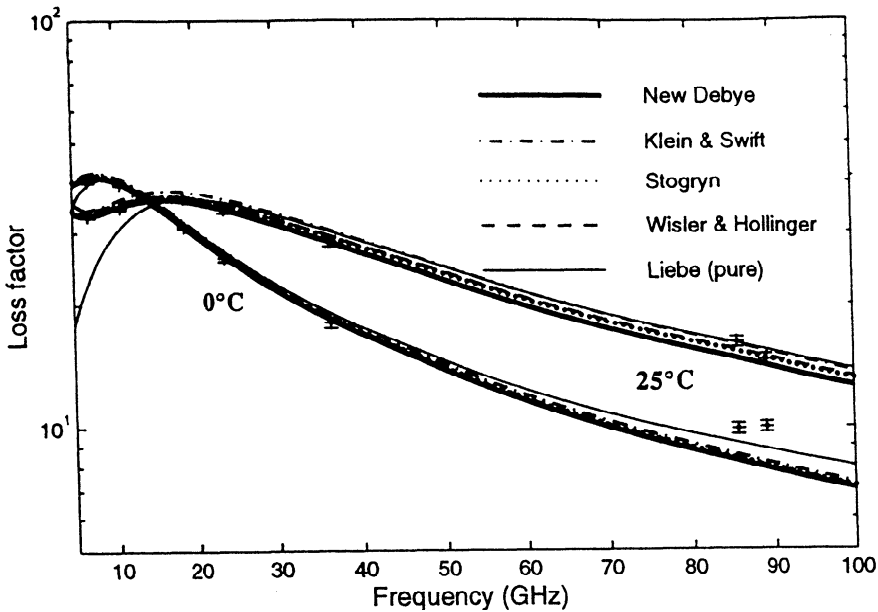


Figure 1. Real part of the dielectric permittivity of liquid water versus frequency at 0°C and 25°C. Simulations for pure water are from the *Liebe et al.* [1991] model, and simulations for seawater (salinity 36‰) are from the revised Debye model (referred to as “New Debye”; equations (1)–(5) in the text) and from the models of *Klein and Swift* [1977], *Stogryn* [1971], and *Wisler and Hollinger* [1977]. Measurements with error bars are at multifrequency imaging microwave radiometer (MIMR) frequencies and at 85.5 GHz [*Ellison et al.*, 1996a].

ments are necessary to allow some extrapolation or interpolation up to 100 GHz with a sufficient degree of confidence. This, unfortunately, was beyond the frame of the measurement campaign. However, some additional measurements have been conducted with the ABmm analyzer at 85.5 GHz, which is the high-frequency channel of the special sensor microwave imager (SSM/I) [*Ellison et al.*, 1996a]. These are only preliminary results at the moment. Since it is highly probable that the permittivity is independent of the salinity over the range 20–40‰ at this high frequency, the measurements were performed on a single seawater sample, at four temperatures (−2°, 12°, 20°, and 30°C) only, which does not justify any interpolation better than linear. The real and imaginary parts of the complex permittivity of seawater at 85.5 GHz are finally given by

$$\epsilon' = 7.6231 + 0.096296T \quad (7a)$$

$$\epsilon'' = 9.8636 + 0.24609T \quad (7b)$$

with a precision of 3%.

3. Comparison With the Literature

All the existing models for seawater and NaCl solutions are based on a single Debye formulation derived from the same rather old measurements (see section 1). Even now, *Klein and Swift* [1977] are still the most quoted source in radiative transfer theories [*Wentz*, 1983; *Guissard and Sobieski*, 1987; *Sasaki et al.*, 1988; *Rosenkranz*, 1992; *Petty and Katsaros*, 1994], although they recommended care using their model at frequencies above 10 GHz. Further experimental investigations have been reported in the literature. From a free wave reflection method, *Blue* [1980] determined the permittivity of pure water, NaCl solution, tap water, seawater, and ice in the short millimeter wavelength region between 97 and 184 GHz, at temperatures ranging from 0°C to 50°C. Unfortunately, only numerical data at 20°C are given. Recently, *Buchner et al.* [1994] reported upon permittivity measurements at a single temperature (25°C), over a large frequency range (0.5–89 GHz). However, this concerns NaF and KF solutions only, which are negligible in seawater. A comparison of the new

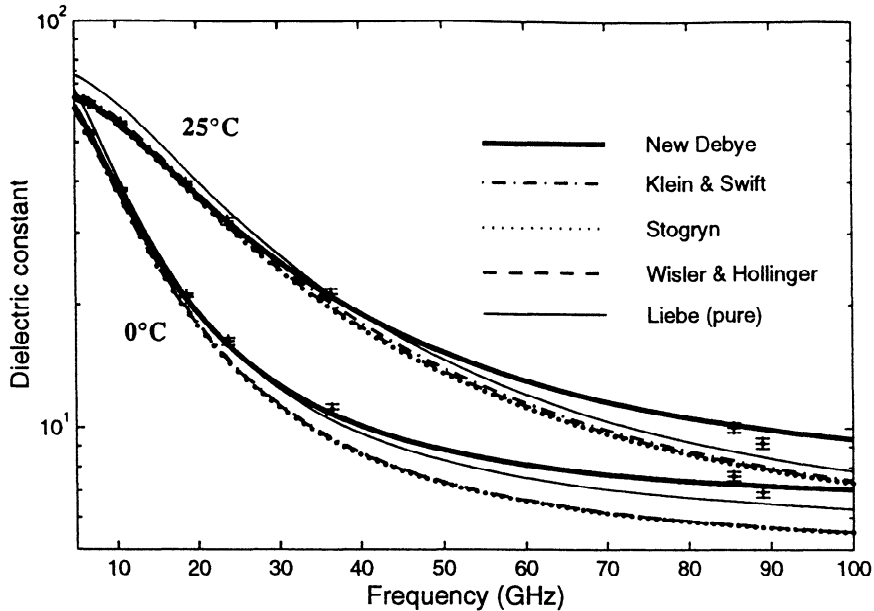


Figure 2. Imaginary part of the dielectric permittivity of liquid water versus frequency at 0°C and 25°C. Same definitions as Figure 1.

permittivity functions with the available literature is presented in Figures 1 and 2.

As already stressed in section 2, the agreement between the predictions provided by the regression fits specifically derived for the MIMR channels and by the revised Debye formulation is limited to frequencies less than 40 GHz. The permittivities predicted by the different single Debye expressions are consistent up to about 10 GHz, while some disparity occurs at higher frequencies between the new model and the older references [Stogryn, 1971; Wisler and Hollinger, 1977; Klein and Swift, 1977]. This mostly concerns the real part of the permittivity, at low temperature (see Figure 1). For example, the dielectric constant ϵ' , as given by the revised Debye model, is actually larger than Klein and Swift's [1977] prediction by 7% at 20 GHz and 0°C; 16% at 40 GHz and 0°C (against 5% only at 25°C); and 27% at 90 GHz and 0°C (23% at 25°C). As illustrated in Figure 2, the dielectric loss factor ϵ'' estimated by the revised Debye model is consistent with Stogryn's estimation up to 100 GHz (within 4%) whatever the temperature but is substantially lower than the Klein and Swift prediction in warm sea condition, from about 5% at 20 GHz, 7% at 40 GHz, and 17% at 90 GHz.

With few frequency measurements the Debye assumption enables the extraction of the relaxation

time, the static dielectric constant, and the so-called dielectric constant at infinite frequency. However, with only two or three frequencies, as is the case for the available models, the resulting Debye parameters are very sensitive to experimental errors in the permittivity measurements. At frequencies higher than about 20 GHz the dominant sources of errors on the dielectric constant are the relaxation time τ and the high-frequency limit ϵ_∞ . Since all the models provide broadly the same τ , the observed discrepancy is mostly related to ϵ_∞ . The lack of measurements led most of the authors to adopt the same approximation for this parameter, which is often supposed to be constant. As an example, ϵ_∞ is fixed at 4.9 by Klein and Swift [1977] with an uncertainty of $\pm 20\%$. Such an error has significant impact on the permittivity as modeled by Klein and Swift. An error of $+20\%$ on ϵ_∞ leads, for instance, to a difference of $+11\%$ and $+17\%$ in ϵ' at 0°C, for the frequencies 40 and 90 GHz, respectively, and to a difference of -11% in ϵ'' at 25°C and 90 GHz. However, a potential temperature dependence of this parameter is still controversial, even regarding the sign of the temperature gradient [Ulaby et al., 1986]. From the new measurements between 3 and 20 GHz, ϵ_∞ is found to range between 6 and 9, depending on the temperature. Moreover, this dependence is not monotonic: ϵ_∞ has

a negative temperature dependence up to about 15°C, followed by a positive gradient at higher temperature. It is worth recalling that this parameter has no real physical meaning since it is not effectively measured at “infinite” frequency. It is introduced to provide the best fit on the data for the Debye function. Nevertheless, its impact on the spectral behavior of the dielectric constant is far from negligible at frequencies higher than X band, as previously noted by *Klein and Swift* [1977].

At 89 GHz the Debye extrapolations deviate significantly from the ABmm measurements by more than 10%, which is much higher than the measurement uncertainty. There are two possible causes for this departure: Either the experimental data are wrong, or the theoretical model is not adequate. In order to test the experimental method the permittivity of pure water was measured at 90 GHz and compared with the independent data reported by *Richards and Sheppard* [1991] at 0°, 20°, 25°, and 30°C. The ABmm values were always found to be within the experimental error claimed by these authors (3–4%). Other measurements for pure water were performed with the ABmm analyzer at frequencies close to 89 GHz and at temperatures for which there are available data in the scientific literature. The comparison with the best estimate from the worldwide database and interpolation scheme [*Ellison et al.*, 1996b] provided similar results. As a consequence, the observed discrepancy is more likely due to the inadequacy of the single Debye relaxation theory at millimeter frequencies. The departure from Debye behavior may be attributed to the influence of a second relaxation process. This was also suggested by recent investigations reporting on the necessity of an additional Debye relaxation term in order to account for the permittivity of pure water at 70 GHz in the temperature range 0.3°–50°C [*Grant et al.*, 1981] and for frequencies between 40 and 89 GHz at 25°C [*Barthel et al.*, 1991]. This behavior is well illustrated in Figures 1 and 2. In view of atmospheric propagation studies, *Liebe et al.* [1991] proposed a new expression for the dielectric permittivity of pure water in the frequency range 1–1000 GHz, which accounts for two Debye relaxation processes. Predictions from this model, as shown in Figures 1 and 2, deviate from Debye behavior, especially at low temperature, in the range 40–100 GHz. Since the effect of the salinity on the dielectric permittivity of seawater is much reduced at millimeter frequencies, it is possible to compare (qualitatively at least) the results for pure

water and seawater. The experimental values for seawater at 89 GHz being much closer to the double Debye predictions than to the standard Debye calculations, this can be interpreted as a further indication that the double Debye assumption prevails for seawater, too.

In order to test the relevance of the new permittivity measurements versus radiometric data, the interpolation functions (equations (1)–(7)) have been applied to a radiative transfer model. Passive microwave responses of the ocean have been simulated and compared with measurements for different experimental configurations. The results are discussed in the next section.

4. Application to the Radiative Transfer Theory

4.1. The Data Set

Satellite radiometric observations have been collected over the North Atlantic, between October 8 and November 16, 1993, from the along-track scanning radiometer-microwave (ATSR/M) on board the European satellite ERS 1, from the TOPEX/POSEIDON microwave radiometer (TMR), and from SSM/I on board the polar orbit DMSP satellites F10 and F11. The ATSR/M operates at 23.8 and 36.5 GHz, at -1.9° and 2.5° along-track from nadir, respectively, while TMR is a perfect nadir-viewing instrument, operating at 18, 21, and 37 GHz. All these channels are observed in vertical polarization. The footprint diameter of TMR decreases from 45, 37, and 23 km at 18, 21, and 37 GHz, respectively, while it is the same for the two ATSR/M channels (21 km). Brightness temperature images at 19.3, 22.2, 37, and 85.5 GHz for both vertical and horizontal polarizations (except the 22.2-GHz channel, which is only observed in vertical polarization) were extracted from four SSM/I orbits on October 10, 17, 27, and November 6, 1993. The orbital characteristics of this instrument are quite different than the previous ones. SSM/I is a conically scanning radiometer which observes the Earth's surface at constant incidence angle of 53° with a cross-track swath width of 1394 km. The spatial resolution decreases from approximately 56, 45, 33, and 14 km with increasing frequency. The internal calibration of the three instruments is performed by means of a cold-sky reflector and of an internal reference load. In any case, however, the in-flight calibration of such spaceborne radiometers requires the use of some radiative transfer modeling. Hence the absolute error

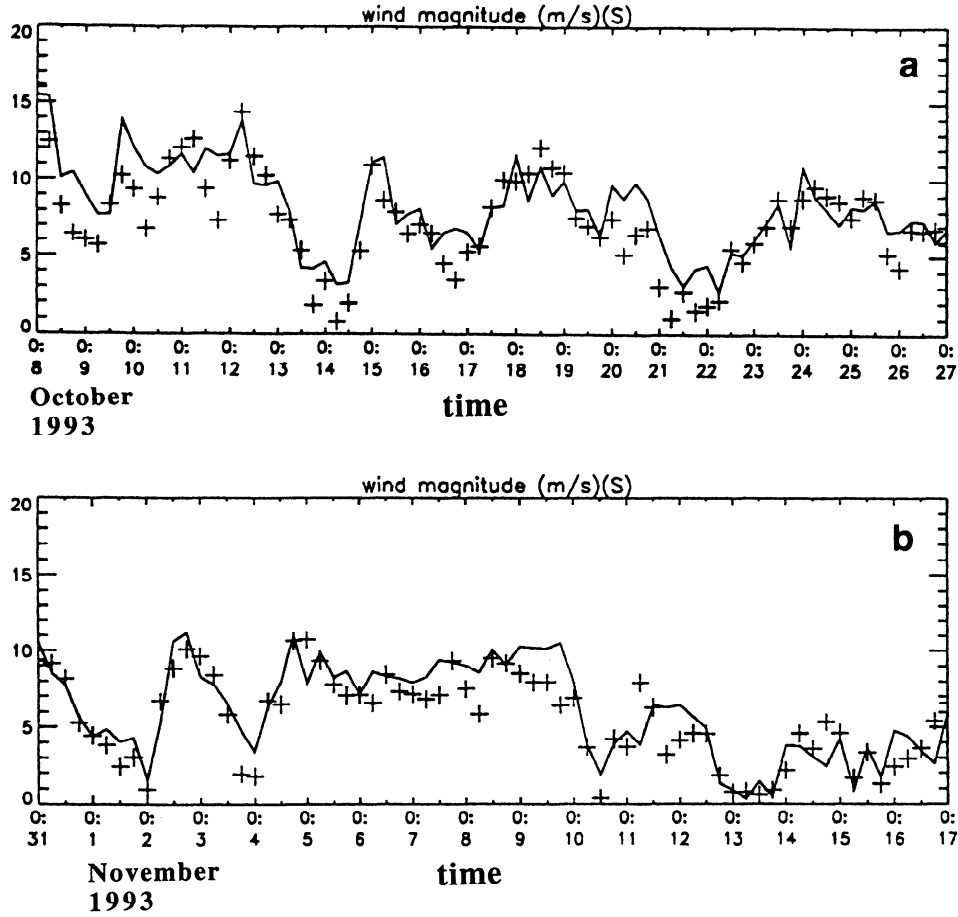


Figure 3. Comparison of the wind speeds (in m/s) versus time from ship measurements (plus signs, 16-m altitude) and from European Centre for Medium-Range Weather Forecasts (ECMWF) analyses (solid line, 10-m altitude) at the grid points where the ship lies, during the SEMAPHORE experiment: (a) between October 8 and 27, 1993, and (b) between October 31 and November 17, 1993.

in the brightness temperature must be considered only as a rough estimation of the calibration quality. It is estimated to be within ± 3 K for ATSR/M [Eymard et al., 1996a] and SSM/I [Hollinger, 1991], while the TMR open-sea brightness temperature accuracy is claimed to be ± 1.5 K [Ruf et al., 1994].

Furthermore, the SEMAPHORE experiment (Structure des Échanges Mer-Atmosphère, Propriétés des Hétérogénéités Océaniques: Recherche Expérimentale) [Eymard et al., 1996b], which took place near the Azores islands in 1993, offered us the opportunity to get and validate outputs of the European Center for Medium-Range Weather Forecast (ECMWF) model over the North Atlantic during October and November 1993. Using buoy and ship local measurements performed southeast of the

Azores, ECMWF global fields of near-surface (10-m altitude) wind speed as well as atmospheric profiles of temperature and humidity were tested. These meteorological analyses are generated every 6 hours on a grid having a spatial resolution of 1.125° in latitude and longitude. Comparisons between ship measurements (wind from an instrumental mast, humidity profiles from radio soundings) and ECMWF values at the grid point in which the ship lies are presented in Figures 3, 4, and 5. Figure 3 shows a good overall agreement in surface wind magnitude versus time between the ship values (at 16 m) and the ECMWF predictions, in average over the experiment duration. The contour lines of humidity profiles are plotted for the ship (Figures 4a and 5a) and for the model (Figures 4b and 5b) for October and November 1993,

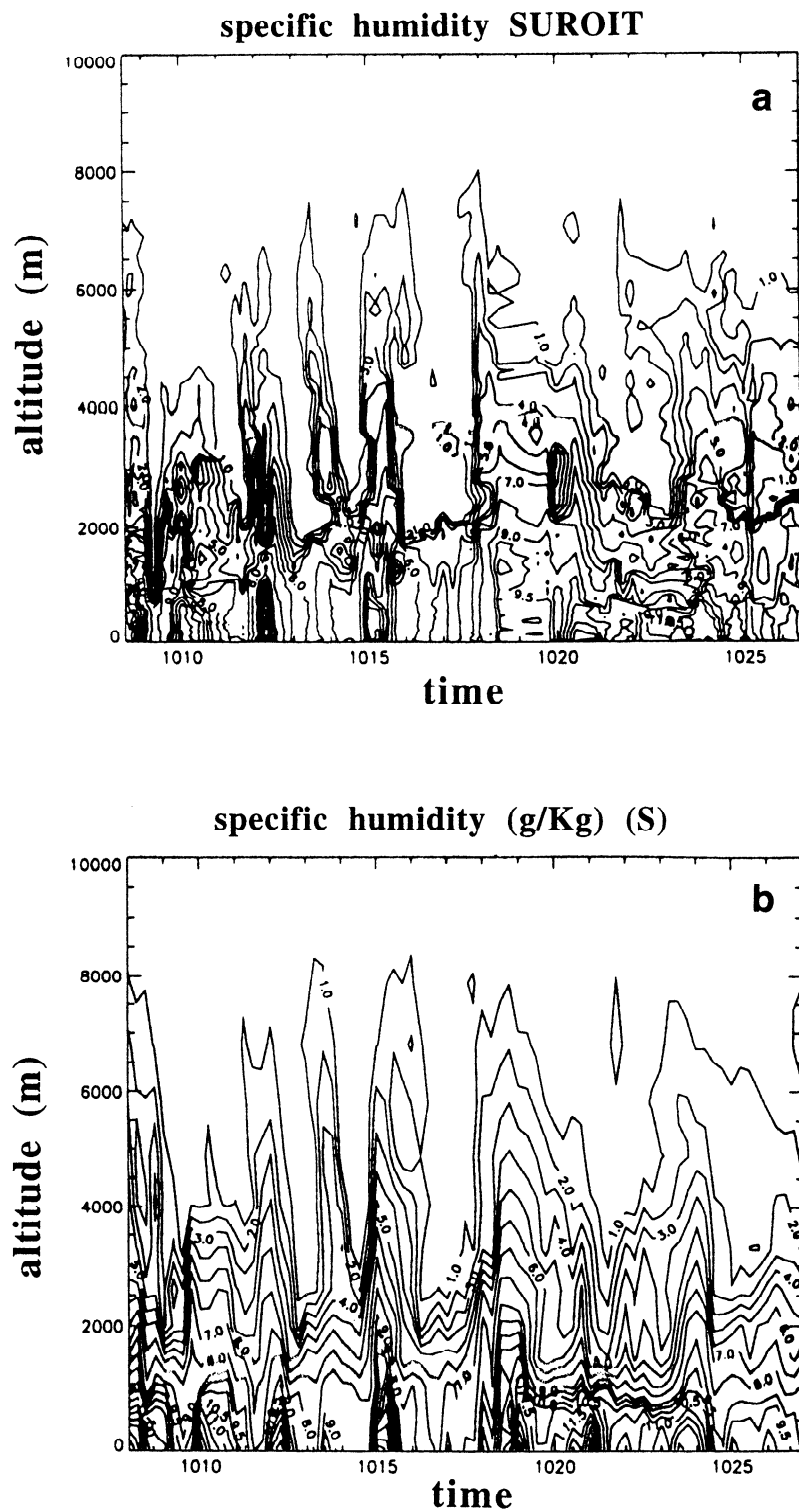


Figure 4. Contour lines of humidity profiles (in g/kg) versus time during the SEMAPHORE experiment. Comparison between (a) ship radio soundings and (b) ECMWF analyses at the points where the ship lies, between October 8 and 27, 1993.

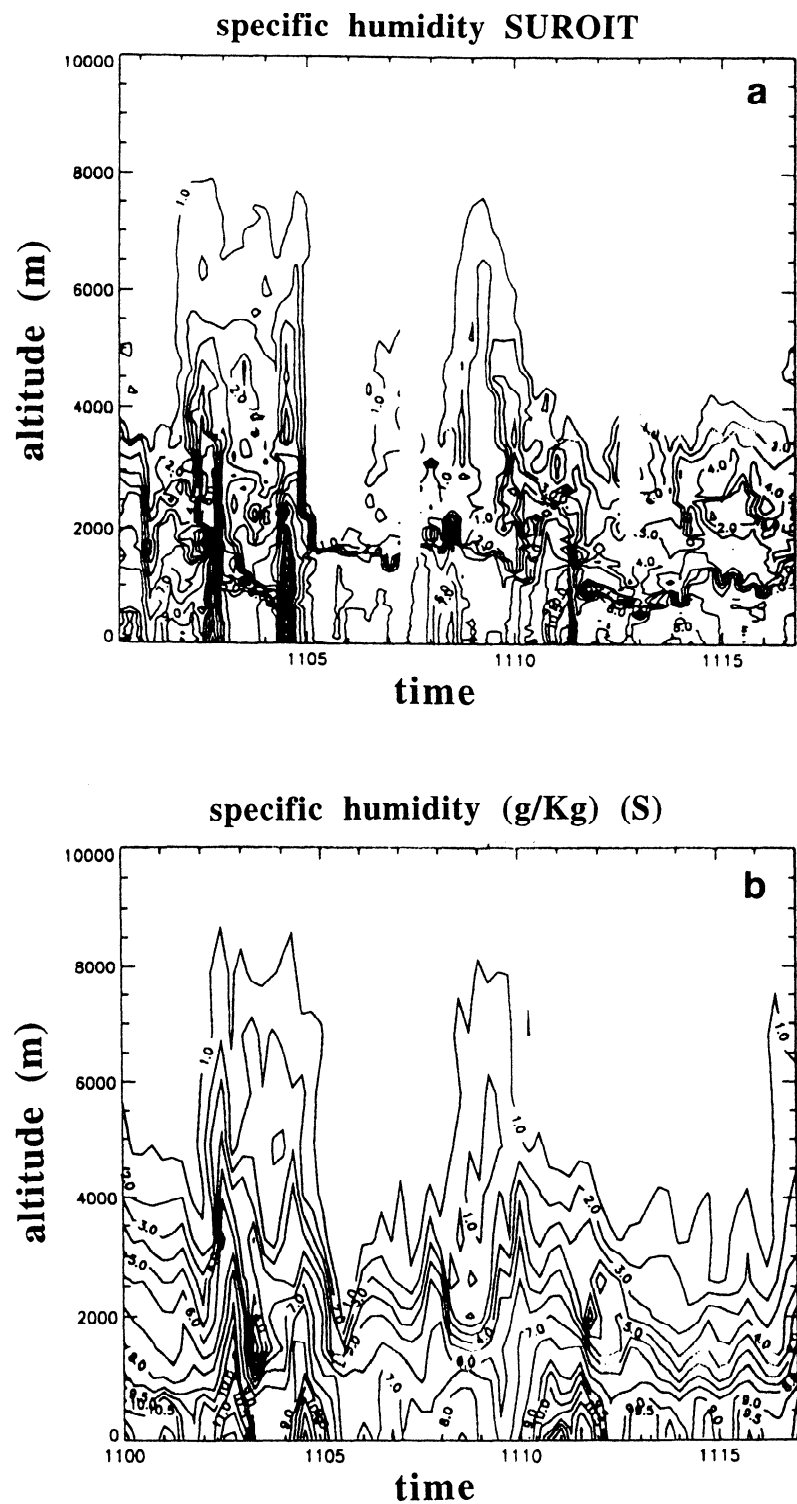


Figure 5. Same as Figure 4 but during the period October 31 to November 17, 1993.

respectively. In Figures 4 and 5 we still note a good agreement in the mean evolution, and only details are significantly different. The same feature occurs with temperature profiles (not shown). In particular, it is clear that a model with 31 levels in vertical cannot reproduce correctly the fine-scale structures near the surface and at the top of the boundary layer, where strong gradients often occur. In spite of these small-scale discrepancies, the model provides a correct description of the atmospheric structures in the experimental region. Since we are not limited to this region only in our investigation, we may extrapolate the results of this comparison and consider the ECMWF model as an adequate representation of the atmospheric characteristics in surface wind, temperature, and humidity fields. The local errors should therefore appear as a noise rather than a bias when making comparisons with satellite measurements over the North Atlantic.

In addition to the satellite data, we took advantage of measurements collected by the microwave airborne radiometer and scanning system (MARSS) flying on the C-130 aircraft of the U.K. Meteorological Office. Since 1990, the MARSS has taken part in several international experiments, which aimed at analyzing the gaseous absorption and the radiative and microphysical properties of the clouds, as well as the surface emissivity, to prepare for the advanced microwave sounding unit (AMSU). The MARSS is a two-channel radiometer operating at 89 and 157 GHz, with a rotating mirror which scans every 3 s both upward and downward, between -40° and $+40^\circ$ nominally, along the aircraft track. Absolute calibration of the instrument is realized in flight using two internal calibration targets. External sources of known brightness temperatures, such as liquid nitrogen on ground or high-level zenith radiation, are also used to achieve full accurate calibration [Hewison, 1991; Jones et al., 1993]. The instrument only views one polarization per channel for each scanning position, which is governed by the orientation of the rectangular section of the waveguide between the feed horn and the mixer.

The data used in this investigation come from well-documented observation campaigns in 1990 and 1991, offering a wide range of atmospheric and sea surface conditions [English et al., 1994; Guillou et al., 1996]. Mean values of brightness temperatures at 89 GHz, within ± 2 K, were recorded on board the aircraft during straight flights at constant and low height for effective incidences ranging between 12°

and 45° from nadir, together with atmospheric and surface parameters. The sea surface temperature was measured to within ± 0.3 K by an infrared radiometer sensor, while equivalent neutral wind speeds (at 10 m) were inferred with a precision of ± 2 m/s from the aircraft velocity combined with an inertial navigation system.

4.2. Surface and Atmosphere Radiative Transfer Modeling

The sea surface brightness temperature in microwaves is related to the complex permittivity of seawater through the definition of its emissivity. If the surface fills a flat half-space at local thermodynamical equilibrium, the emissivity at incidence θ from the vertical is defined by

$$\epsilon_p = 1 - R_p \quad (8)$$

where p is the polarization of the signal, horizontal (H) or vertical (V), and R_p is the square of the Fresnel reflection coefficient for polarization p :

$$R_H = \left| \frac{\cos \theta - \sqrt{\epsilon - \sin^2 \theta}}{\cos \theta + \sqrt{\epsilon - \sin^2 \theta}} \right|^2 \quad (9)$$

$$R_V = \left| \frac{\epsilon \cos \theta - \sqrt{\epsilon - \sin^2 \theta}}{\epsilon \cos \theta + \sqrt{\epsilon - \sin^2 \theta}} \right|^2$$

However, in natural sea conditions, this definition becomes too simplistic. The action of the wind on the surface leads to significant modifications of both the scene-average Fresnel emissivity and the angular weighting function of diffusely reflected sky emission. The surface roughness is composed of a large number of wave components, whose dimensions, spatial distribution, and temporal variation are described by statistical laws, although it is obvious that some particular features like foam, spray, and bubbles cannot be properly accounted for in such a description. The signal received by a spaceborne radiometer observing the ocean at frequency ν , polarization p , and incidence θ from nadir is calculated from the radiative transfer equation. When scattering by hydrometeors is negligible (as it will be assumed here), the brightness temperature at satellite level can be written as

$$T_B = (\epsilon_p T_s + T_{\text{scat}}) e^{-\tau \sec \theta} + T_{\text{up}} \quad (10)$$

where T_s is the sea surface temperature, T_{scat} is the reflected (polarized) component of the downward

atmospheric radiation, τ is the atmospheric opacity, and T_{up} is the upwelling brightness temperature of the atmosphere.

Several theoretical models have been proposed to predict the microwave emission and scattering properties of a wind-roughened sea [Stogryn, 1967; Wilheit, 1979; Wu and Fung, 1972; Wentz, 1975; Guissard and Sobieski, 1987; Fung and Tjuatja, 1993]. At present, however, a fully adequate modeling is still difficult to assess. For the present purpose, we adopted a geometric optics approach, stemming from Stogryn's [1967] and Wilheit's [1979] developments. A complete description of this model is given by Guillou *et al.* [1996]. Basically, the sea surface is described by a series of reflecting plane facets characterized by a bidirectional slope distribution, as given by Cox and Munk [1954]. Each individual facet is assumed to be infinite in front of the wavelength, and irregularities small or comparable to the wavelength are ignored. The scattering component of the brightness temperature results from the integration of the sky radiation over the upper hemisphere, and the elementary contribution of each facet to this component is computed from the Fresnel relations at local incidence. Foam effects are taken into account in the calculations in a very simplistic manner because of the lack of adequate modeling of this contribution for any experimental configuration up to now. For each facet the apparent temperatures in vertical and horizontal polarizations are modified by including the fractional foam coverage as defined by Monahan and Lu [1990], and the foam emissivity is assumed to be 1.

Under clear-sky conditions the atmospheric contribution within the microwave domain is governed by attenuation and emission due to water vapor and oxygen. It is calculated by assuming a horizontally infinite plane parallel atmosphere, by means of gaseous absorption coefficients, as a function of pressure, temperature, and humidity content, together with spectroscopic parameters. Various gaseous absorption models available in the literature were tested on measurements from atmospheric field experiments in the microwave windows [English *et al.*, 1994; Guillou, 1994]. Although some underestimation of the theoretical prediction still prevailed in the low-frequency wing of the 22.2-GHz water vapor line, superiority of the Liebe *et al.* [1993] model up to 90 GHz was recognized. This model will be used in the following to simulate both the atmospheric opacity and the upward and downward propagating brightness temperatures from meteorological profiles.

4.3. Comparison method

For comparison with the satellite data, collocated and nearly synchronized (within ± 2 hours) ECMWF analyses have been applied to the radiative transfer model to simulate brightness temperatures as seen by ATSR/M, TMR, and SSM/I. Clear-air data only were retained after applying microwave algorithms of integrated liquid water on the measurements. These algorithms (see the appendix) were derived from a method detailed by Eymard *et al.* [1996a], the validity of which is discussed by Gérard and Eymard [this issue]. When several satellite measurements were included in one grid mesh (as is often the case for SSM/I), these measurements were averaged. At the end of this stringent procedure, there remained a set of 444, 547, and 1365 data points that were used from the ATSR/M, TMR, and SSM/I orbits, respectively, to be compared with the radiative transfer predictions.

The validation procedure associated with the airborne data is quite different. The downwelling brightness temperatures used by the radiative transfer model stem from the MARSS measurements when looking at the sky and corrected for the thin slab of atmosphere between the flying altitude (30–165 m) and the sea surface. The comparison between the measurements and the simulations is performed at sea level, after correcting the downward data for the same atmospheric contribution. This contribution was calculated from regression formulas relating the optical depth of the atmospheric slab and the water mass mixing ratio measured at the flight altitude. Observations that were contaminated by inhomogeneous clouds were rejected, as well as data polluted by Sun glitter in the field of view. A total of 1004 climatologically representative data were finally extracted.

In order to test the impact of the dielectric permittivity on the sea surface emissivity modeling, calculations using the new permittivity model (Debye formulation up to 40 GHz and interpolation functions at 85.5 and 89 GHz) and the classical model of Klein and Swift [1977] will be compared.

4.4. Results

The comparison between measured and simulated brightness temperatures using the Klein and Swift [1977] dielectric model is presented in Table 1 from a statistical point of view. The ATSR-M and the TMR configurations exhibit comparable results: The mean deviations are within the error bars of the instruments, despite some slight underestimate of the model for the highest brightness temperatures. The

Table 1. Statistical Results of the Comparisons Between Radiometric Data and Simulations Using the *Klein and Swift* [1977] Dielectric Model

Instrument	Frequency, GHz	Mean, K	s.d., K	<i>R</i>	Regression Coefficient	
					<i>a</i>	<i>b</i>
ATSR/M	23.8	1.3	5.5	0.94	0.892	17.1
	36.5	2.2	2.7	0.91	0.914	11.8
	18	0.9	2.3	0.92	0.914	10.8
TMR	21	1.7	4.9	0.94	0.918	11.9
	37	1.4	2.9	0.89	0.873	19.5
	19V	5.3	2.9	0.96	0.873	19.6
	19H	5.4	5.2	0.94	0.864	12.4
	22V	3.9	4.5	0.97	0.929	11.8
	37V	1.0	2.3	0.94	0.896	21.4
SSM/I	37H	3.8	4.4	0.92	0.935	6.0
	85V	0.0	3.0	0.96	0.933	17.1
	85H	4.3	7.2	0.95	1.010	-6.6
	89	1.4	2.6	0.96	0.873	23.9

The mean and the standard deviation refer to the differences between measurements and simulations. The *a* and *b* coefficients are the slope and the offset, respectively, in the linear regression of simulated versus measured brightness temperatures. *R* is the associated correlation coefficient.

low-frequency channels of SSM/I show the same qualitative behavior (high brightness temperatures greater than model predictions), but the mean deviations are more important (more than 5 K at 19 GHz), exceeding the error bars of the instrument except in the channel 37V. At 85 GHz the simulations fit the observations rather well in vertical polarization, while a significant positive bias of 4.3 K is found in horizontal polarization. Finally, on average over the whole meteorological data set, the scatterplot of simulated versus radiometric airborne data at 89 GHz provides a consistent agreement (mean deviation 1.4 K), within the absolute accuracy of the MARSS (± 2 K in calibration; see section 4.1), but a least squares slope much lower than unity.

As expected, the application of the new dielectric permittivity functions to the radiative transfer model affects the results of the comparison with the satellite and airborne observations. The corresponding statistical parameters are listed in Table 2. As an example, Figures 6 and 7 show the scatterplots of calculated versus observed brightness temperatures at 37 GHz, for each satellite configuration and dielectric model.

At frequencies less than 40 GHz the revised Debye model provides a better overall agreement with the data than the *Klein and Swift* [1977] model. The most significant difference between the two permittivity pre-

dictions is obtained at 37 GHz in the nadir-viewing channels of ATSR/M and TMR (means deviations reduced by 2.1 and 2.3 K, respectively). This difference is less pronounced at 53° incidence, especially in horizontal polarization. A similar polarization effect is observed in the SSM/I channels 19V and 19H, the mean deviations being reduced by 1.6 and 1 K, respectively.

The results obtained at 85.5 and 89 GHz are quite different. While no significant effect is pointed out at 85.5 GHz from the use of the new permittivity function, as compared with *Klein and Swift's* [1977] predictions, the use of the permittivity function derived at 89 GHz leads to a significant underestimate of the simulations (mean deviation increased by 4.1 K) as shown in Figure 8. However, the regression slopes are improved both at 89 GHz and in the channel 85.5V. Hereinafter we shall discuss these results together with a sensitivity analysis of the radiometric signal to the dielectric permittivity of seawater.

4.5. Discussion

Since the ECMWF fields are statistically correct, the observed discrepancies between model predictions and satellite measurements cannot be attributed to weaknesses of the meteorological model as input of the radiative transfer. However, local forecasting errors due to a lack of measurements occur and introduce errors in the structure of the atmospheric profiles (shifts, intensity inadequacies; see section 4.1).

Table 2. Statistical Results of the Comparisons Between Radiometric Data and Simulations Using the New Dielectric Permittivity Functions

Instrument	Frequency, GHz	Mean, K	s.d., K	<i>R</i>	Regression Coefficient	
					<i>a</i>	<i>b</i>
ATSR/M	23.8	0.0	5.4	0.94	0.887	19.4
	36.5	0.1	2.7	0.91	0.942	9.5
	18	-0.6	2.3	0.92	0.924	11.0
TMR	21	0.3	4.9	0.94	0.916	13.6
	37	-0.9	2.9	0.90	0.901	17.2
	19V	3.7	3.0	0.96	0.873	21.3
	19H	4.4	5.2	0.94	0.863	13.6
	22V	2.7	4.5	0.97	0.921	14.9
SSM/I	37V	-1.0	2.2	0.95	0.919	18.1
	37H	2.3	4.3	0.93	0.944	6.1
	85V	0.5	3.0	0.96	0.978	5.2
	85H	4.8	7.2	0.95	1.029	-11.5
MARSS	89	5.5	2.6	0.96	0.936	7.2

Model is the revised Debye model, as defined by equations (1)–(5) in the text, below 40 GHz; interpolation functions are as defined by equations (6) and (7) at 89 and 85.5, GHz respectively. Definitions are the same as in Table 1.

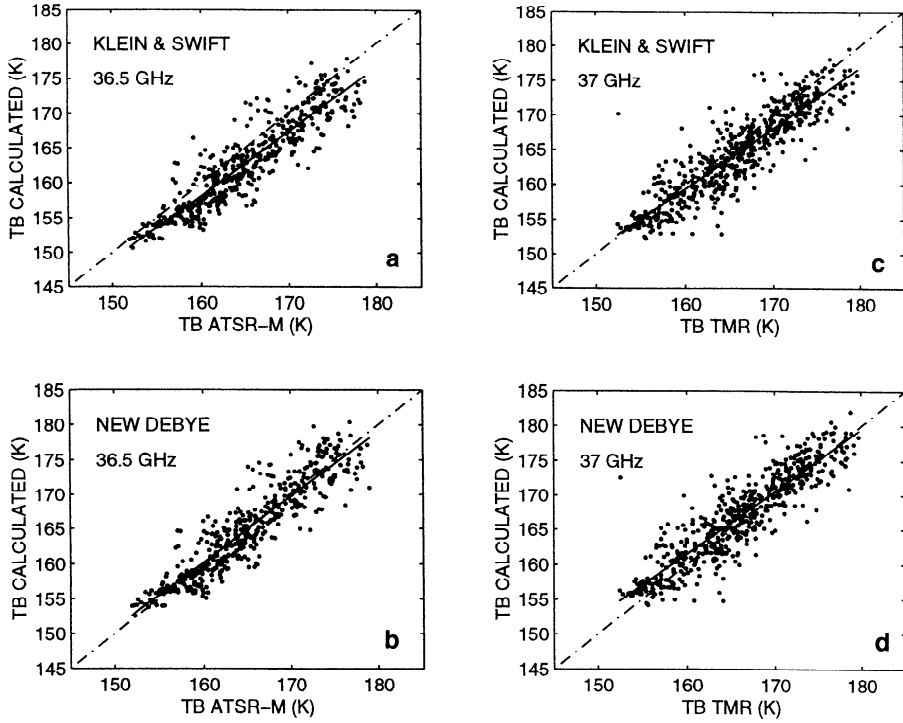


Figure 6. Scatterplots and least squares lines of calculated brightness temperatures versus along-track scanning radiometer-microwave (ATSR-M) and TOPEX/POSEIDON radiometer-microwave (TMR) data at 36.5 and 37 GHz, respectively. (a and c) Comparison between the *Klein and Swift* [1977] dielectric model predictions and (b and d) the revised Debye model (referred to as “new Debye”) predictions.

This effect likely contributes to the large standard deviations obtained in the water vapor channels (sensitivity to errors in humidity profiles). A simple calculation from the radiative transfer equation also shows that the sensitivity of the brightness temperature to the atmospheric opacity and to the wind speed is more pronounced in horizontal than in vertical polarization. This probably explains the larger standard deviations obtained at 19H, 37H, and mostly 85H, this millimeter frequency being sensitive to both water vapor (through the continuum) and wind speed fluctuations.

Numerical tests were performed at MIMR frequencies to analyze the sensitivity of the radiometric signal to the complex permittivity of seawater, as defined by the new model. In order to maximize this quantity, the calculations were conducted at sea level by using a subarctic atmosphere [Ulaby *et al.*, 1986], whose contribution to the radiation is weak. The results indicate that the real part ϵ' and the imaginary part ϵ'' have comparable effects on the brightness temperature at 6.8 and 10.65 GHz, while the sensitivity to ϵ' becomes negligible at 36.5 GHz, as compared

with the sensitivity to ϵ'' . A polarization dependence, to ϵ'' principally, is also indicated. As the incidence angle increases from nadir to about 50° , the sensitivity of the radiometric signal decreases in horizontal polarization for frequencies less than 40 GHz, while it remains constant in vertical polarization. On the other hand, at 89 GHz, it is reduced in both polarizations, especially at low temperature.

When examining the specific case of the MIMR vertical channels at 50° incidence, we find, as shown in Figure 9, that the sensitivity of the brightness temperature to ϵ' diminishes with increasing frequency from about 0.4 to 0.1 K per unit of ϵ' at 0°C (from 0.6 to 0.2 K per unit of ϵ' at 25°C), while its sensitivity to ϵ'' increases with increasing frequency from 0.6 to 3.8 K per unit of ϵ'' at 0°C (0.4–3 K per unit of ϵ'' at 25°C). If we define the absolute error on the radiometric signal relative to the complex permittivity ϵ in the following manner,

$$\Delta T_B = \max \left[\left| \frac{\partial T_B}{\partial \epsilon'} \right| \Delta \epsilon', \left| \frac{\partial T_B}{\partial \epsilon''} \right| \Delta \epsilon'' \right] \quad (11)$$

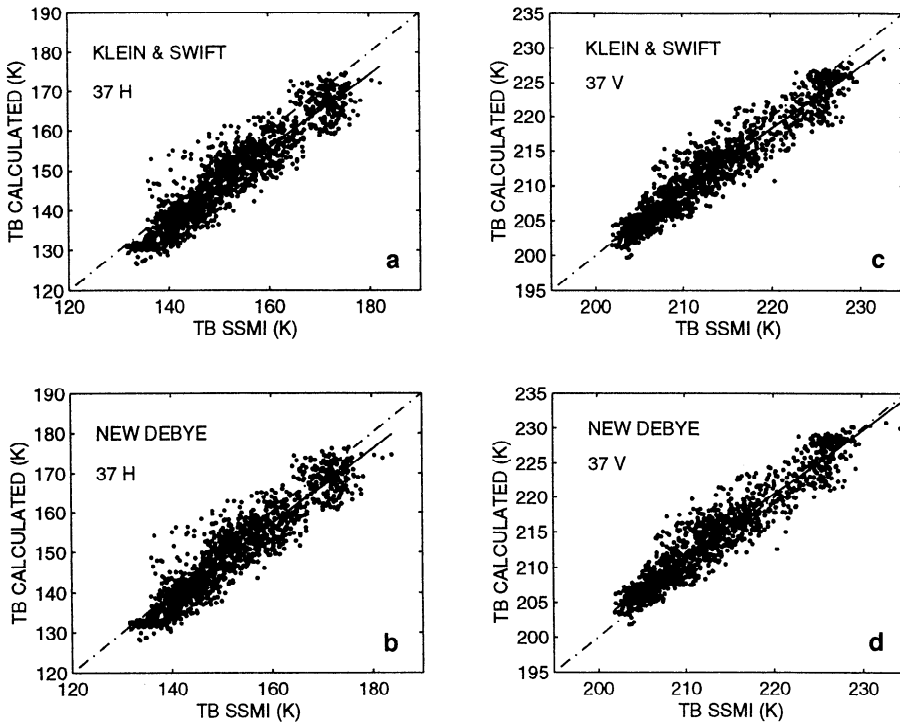


Figure 7. Scatterplots and least squares lines of calculated brightness temperatures versus special sensor microwave imager (SSM/I) data at 37 GHz. Comparison between the *Klein and Swift* [1977] dielectric model predictions for (a) horizontal polarization, (c) vertical polarization, and (b and d) the revised Debye model (referred to as “new Debye”) predictions.

then this leads to absolute errors on the radiometric signal, given the estimated errors on the permittivity measurements (see section 2), within 0.5 K at the three lowest frequencies, 1 K at 23.8 GHz and 1.5 K at 36.5 and 89 GHz. According to the MIMR radiometric specifications, these errors, which will be re-

duced at satellite level by the atmospheric transmission term, are well within the absolute accuracy of the MIMR instrument (1 K at 6.8 and 10.65 GHz and 1.5 K at higher frequency).

4.5.1. Frequency range 0–40 GHz. These sensitivity tests justify the improvement of the statistical

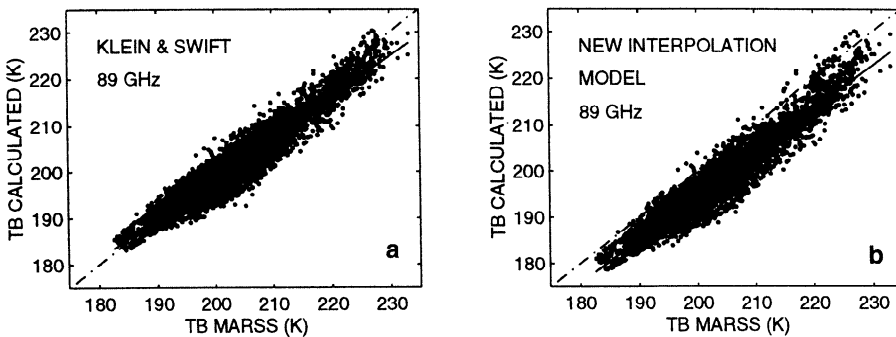


Figure 8. Scatterplots and least squares lines of calculated brightness temperatures versus microwave airborne radiometer and scanning system (MARSS) data. Comparison between (a) the *Klein and Swift* [1977] dielectric model predictions and (b) the new interpolation function at 89 GHz, as defined by equation (6).

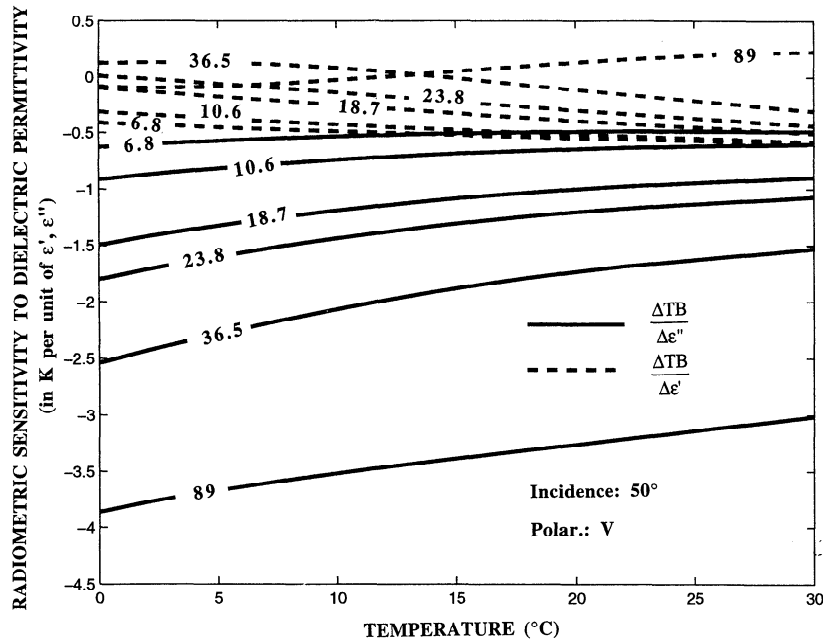


Figure 9. Radiometric sensitivity to the real part ϵ' (dashed line) and to the imaginary part ϵ'' (solid line) of the complex permittivity versus temperature at MIMR frequencies. Shown are numerical simulations at 50° incidence, in vertical polarization, using the revised Debye model (equations (1)–(5)), salinity fixed at 35‰ below 40 GHz, and the new interpolation function (equation (6)) at 89 GHz.

mean deviations provided by the revised Debye model below 40 GHz and its higher impact in the vertical than in the horizontal channels of SSM/I. This can be easily demonstrated by a simple calculation at sea level. The loss factor predicted by the revised Debye model is lower than the one defined by *Klein and Swift* [1977], as previously stressed in section 3. It is also almost entirely responsible for the radiometric sensitivity to the dielectric permittivity above 18 GHz. Hence a decrease of about 4% in the loss factor, as defined by Klein and Swift at 18–19 GHz, results in an increase in the brightness temperature, in vertical polarization and whatever the observing angle, of about 1.5 K on average over the whole temperature range. Similarly, a decrease within 5–7% in the loss factor at frequencies close to 22 GHz and at 37 GHz leads to an average increase of the radiometric signal of about 2.1 and 2.5 K, respectively. In horizontal polarization, around 53° incidence, the average differences between the *Klein and Swift* [1977] and the new Debye predictions are only within 0.9 K at 19 GHz and 1.9 K at 37 GHz. At satellite level, all these average differences are reduced, especially in the water vapor channels at oblique angle, due to the wet tropospheric attenuation. In particular, this is why the

water vapor channels appear much less affected by the use of the revised Debye model than the liquid water channels.

In comparisons between satellite data and radiative transfer simulations, any calibration specific problem is more easily detected at low brightness temperatures, where errors related to the model used to calibrate the instrument in flight are limited (both atmospheric opacity and wind-induced roughness effects are reduced). This is especially true for Dicke radiometers like TMR and ATSR/M. In light of this feature, no particular calibration problem is evidenced from our results. The discrepancies between the data and the theoretical predictions using *Klein and Swift's* [1977] permittivity affect more specifically the highest values, and the application of the revised Debye model leads generally to an improvement of the linear regression slopes (or at least no significant degradation). Although the statistical results listed in Tables 1 and 2 should not be taken literally, given the way of calibrating satellite radiometric data, this last behavior leads to favoring the new dielectric model, as opposed to the older ones. As already underlined in section 2, the retrieval of the new Debye parameters was based on a sharp temperature sampling

between 3 and 20 GHz, resulting in very accurate parameters. This, no doubt, contributes to the overall improvement of the simulations, when coupled to the new dielectric model.

In spite of this overall improvement, model deficiencies, particularly in the sea surface roughness treatment, may still be suspected below 40 GHz, where the validity of the geometric optics approach is not guaranteed. In addition to the specular reflection by tilted plane facets, diffraction of microwaves by surface waves having smaller dimensions than the radiation wavelength has been shown to induce significant impact on the radiometric signal at these frequencies [Guissard and Sobieski, 1987; Wu and Fung, 1972; Wentz, 1975]. This contribution possibly accounts for the disagreement observed in the 19H and 19V SSM/I channels, which are the most sensitive to sea surface effects. Nevertheless, we shall not enlarge upon all sources of modeling errors, the aim of this paper being rather to focus on the seawater dielectric aspect.

4.5.2. Millimeter frequencies. Despite the proximity of the frequencies, the divergence observed in the statistical results at 85 and 89 GHz may suggest an inconsistency in the permittivity measurements at both frequencies. This is, however, not apparent from Figures 1 and 2. On the other hand, the MARSS measurements were conducted between 10° and 40° incidence typically from nadir, while SSM/I operates at the constant angle of 53° . As previously stressed in the numerical sensitivity analysis, the sensitivity of the brightness temperature to the dielectric permittivity at 89 GHz decreases with increasing incidence in both polarizations. Hence, at 89 GHz for low temperatures, the radiometric sensitivity to ϵ'' is higher by more than 10% at nadir than at 50° . The resulting variation in brightness temperature at sea level between the two dielectric model predictions, as inferred from Figure 2 and Figure 9, is larger by about 1.5 K at nadir than at 50° . Moreover, the comparisons with the MARSS data are performed at sea level, and the departures between the two model predictions are not weakened by the atmospheric attenuation. However, the water vapor continuum is, to a large extent, responsible for the strong atmospheric attenuation at our millimeter frequencies: The transmission factor can go down 0.4 at 53° incidence in the case of moist and warm atmospheres. As a consequence, extreme deviations of 6 K between the two model predictions at sea level, as is the case in SSM/I configuration for very low sea surface temperatures, can be reduced to

2.5 K at satellite level. Finally, as no difference between the two model predictions is expected at high temperature because of identical values of ϵ'' (see Figure 2), these simple calculations justify the imperceptible repercussion induced by the new permittivity function on the mean deviations at 85 GHz, on average over the whole temperature range, as opposed to the MARSS configuration.

In other respects, the most remarkable results concern the great improvement of the regression slopes at 85.5V and 89 GHz. Again, this behavior leads to favoring the new permittivity measurements, despite the strong positive bias of 5.5 K revealed in the case of MARSS. The Klein and Swift [1977] and the new dielectric expressions differ, among other ways, through their temperature dependence: The temperature gradient of the new permittivity function is indeed less pronounced. It is worth mentioning that the double Debye model of Liebe *et al.* [1991] for pure water exhibits, as well, a much lower temperature gradient than single Debye models. Compared with MARSS data at 89 and 157 GHz, this model proved its superiority to the Klein and Swift formulation at both millimeter frequencies [Guillou *et al.*, 1996]. Our comparisons with airborne and satellite radiometric observations tend to confirm the recent experimental investigations, arguing for the existence of a second "high-frequency" relaxation process that influences the dielectric permittivity of liquid water at millimeter frequencies, even below 100 GHz (see section 3).

However, the strong biases found at 85.5H and 89 GHz are still not elucidated. The SSM/I calibration is based on fittings of the data on radiative transfer predictions using a two-scale sea surface scattering model [Wentz, 1975], which differs from the geometric optics approach by the combination of two scattering processes accounting for the specular reflection of the electromagnetic wavelength by long waves and the diffraction of microwaves by small ripples. In that sense, it is obviously illusive to look for a perfect agreement between our theoretical predictions and the SSM/I data. On the other hand, the MARSS calibration is completely independent of any radiative transfer modeling. Fully accurate calibration of the instrument is achieved in flight every scan (3-s duration) from two reference targets considered as perfectly black and whose temperatures are closely controlled [Hewison, 1991; Jones *et al.*, 1993; Jones, 1991]. Thus errors originating from this calibration procedure should be discarded, and we rather suspect model deficiencies. The gaseous absorption model of

Liebe et al. [1993] has been shown to provide very good agreement when tested on the upward MARSS data at 89 GHz, as well as on zenith and ground radiometric observations at 90 GHz [*Guillou*, 1994]. On the other hand, the choice of the input parameters in the sea scattering model is still questionable, in particular the choice of the slope variance used in the slope probability density function characterizing the series of plane facets. For instance, if we replace the *Cox and Munk* [1954] slope variance by the one derived from the *Bjerkas and Riedel* [1979] sea spectrum in our simulations, the mean deviation at 89 GHz is reduced to 3.2 K, slightly out of the error bars, and the regression slope is even closer to unity (1.0365 instead of 0.9364). This test is very revealing, in that the greatest care must be taken in the interpretation of radiometric satellite data, and all aspects involved in the emissivity and reflectivity properties of the sea surface must be treated separately.

5. Conclusions

Dielectric measurements of seawater covering the range of temperatures and salinities found in the world's oceans have been conducted between 3 and 89 GHz. An improved permittivity model has been derived, based on the standard Debye theory, for remote sensing applications below 40 GHz. Polynomial interpolations, independent of the salinity, have been also developed for specific use at 85.5 and 89 GHz. A radiometric sensitivity analysis showed that within the error estimates of 1% below 20 GHz and of 3% at higher frequencies, the new permittivity measurements yield an accuracy in brightness temperature of at least 0.5, 1, and 1.5 K, respectively, which is highly satisfying regarding the technical improvements in sensitivity and precision expected from the new generation of spaceborne microwave radiometers.

Applied to the radiative transfer equation under clear-sky condition, the revised Debye model provided a better overall agreement in comparison with satellite radiometric data than the commonly used model of *Klein and Swift* [1977], especially at nadir. The statistical mean deviations between measured and simulated brightness temperatures are well within the error bars of the ATSR/M and the TMR instruments. Except for channel 37V, however, the model still underestimates the low-frequency SSM/I data, up to 4.4 K at 19H. The most significant improvement occurs at 37 GHz, both in the least square slopes and in the mean deviations (reduced by

more than 2 K in the liquid water channel of TMR). Divergent, although justified, results have been obtained at millimeter frequencies, in comparison between the new permittivity functions and the Klein and Swift predictions with high-frequency SSM/I data and airborne radiometric measurements at 89 GHz. While no significant effect on the mean deviations has been evidenced at 85.5 GHz, a strong positive bias of 5.5 K has been found at 89 GHz. In return, the linear regression slopes have been much improved in the channel 85.5V and at 89 GHz, suggesting a better adequacy, at millimeter frequencies, of the temperature dependence in the new permittivity functions than in the classical standard Debye equations.

This study aimed at emphasizing the sensitivity of the ocean radiometric signal to the dielectric permittivity model for seawater. The results augur interesting outputs in the interpretation of satellite data. In particular, in-flight calibration of the instruments may be revised, coupled to both adequate treatment of the wind-induced sea surface roughness and the surface emissivity model. The retrieval of cloud liquid water may also be enhanced, especially beyond the lowest integrated contents. This study provided the opportunity to elucidate other questions also. As detailed by *Ellison et al.* [this issue], the conductivity of natural seawater has been found to be 3% lower than the conductivity of NaCl solutions, and the organic content of seawater has been shown to have negligible effect on the dielectric permittivity in the spectral range 3–90 GHz.

However, in order to correctly exploit radar and radiometric data in the frequency range 40–150 GHz, further permittivity measurements of natural seawater are required, with an accuracy of better than 5%, to allow some serious interpolation model for use at any frequency of the microwave spectrum. Such measurements for pure water and seawater are currently in progress at the French laboratory PIOM. More generally, the frequency range from 100 GHz to 1 THz has been only partially explored to date. Both experimental and theoretical investigations should help us understand the physical dielectric properties of liquid water and enlarge upon the field of applications, such as the analysis of the microwave scattering by hydrometeors.

Appendix

Algorithms used to retrieve the liquid water content (LW) (in mg/cm²) from ATSR/M, TMR, and

SSM/I brightness temperatures [Eymard *et al.*, 1996a; Gérard and Eymard, this issue] are the following:

(ATSR/M)

$$\begin{aligned} \text{LW} = & 665.1422 + 77.0217 \ln(280 - TB24) \\ & - 215.5787 \ln(280 - TB36) - 0.4639(U - 7) \end{aligned}$$

where U is the surface wind speed at 10-m altitude, in m/s.

(TMR)

$$\begin{aligned} \text{LW} = & 488.6575 + 23.3452 \ln(280 - TB18) \\ & + 81.5728 \ln(280 - TB21) \\ & - 208.6921 \ln(280 - TB37) \end{aligned}$$

(SSM/I)

$$\begin{aligned} \text{LW} = & 162.7221 - 8.863 \ln(280 - TB19V) \\ & + 107.1356 \ln(280 - TB19H) \\ & + 8.9958 \ln(280 - TB22V) \\ & - 44.5467 \ln(280 - TB37V) \\ & - 104.3607 \ln(280 - TB37H) \end{aligned}$$

Acknowledgments. This work was supported by the European Space Agency under ESTEC/ESA contract, reference 11197/94/NL/CN. The authors thank J. Noll and M. Wintzer from ESTEC/ESA for helpful comments on this work. S. English from the U.K. Meteorological Office is gratefully acknowledged for generously providing us free use of the MARSS data. The authors are also grateful to ECMWF for providing model outputs and to D. Dagorne from ORSTOM Lannion (France) for supplying the SSM/I data during the SEMAPHORE experiment.

References

- Barthel, J., K. Bachhuber, R. Buchner, H. Hetzenauer, and M. Kleebauer, A computer-controlled system of transmission lines for the determination of the complex permittivity of lossy liquids between 8.5 and 90 GHz, *Ber. Busen Ges. Phys. Chem.*, 95(8), 583–588, 1991.
- Bjerkaas, A. W., and F. W. Riedel, Proposed model for the elevation spectrum of a wind-roughened sea surface, *Johns Hopkins Tech. Memo.*, JHU/APL TG 1328, 31 pp., 1979.
- Blue, M. D., Permittivity of ice and water at millimeter wavelengths, *J. Geophys. Res.*, 85(C2), 1101–1106, 1980.
- Buchner, R., G. T. Heffer, and J. Barthel, Dielectric relaxation of aqueous NaF and KF solutions, *J. Chem. Soc. Fraday Trans.*, 90, 2475–2479, 1994.
- Cox, C., and W. Munk, Measurements of the roughness of the sea surface from photographs of the Sun's glitter, *J. Opt. Soc. Am.*, 44, 838–850, 1954.
- Ellison, W., A. Balana, G. Delbos, K. Lamkaouchi, L. Eymard, C. Guillou, and C. Prigent, Study and measurement of the dielectric properties of seawater: Final Report, *ESTEC/ESA Contr. 11197/94/NL/CN*, 1996a.
- Ellison, W., K. Lamkaouchi, and J. M. Moreau, Water: A dielectric reference, *J. Mol. Liq.*, 68, 1–109, 1996b.
- Ellison, W., A. Balana, G. Delbos, K. Lamkaouchi, L. Eymard, C. Guillou, and C. Prigent, New permittivity measurements of seawater, *Radio Sci.*, this issue.
- English, S. J., C. Guillou, C. Prigent, and D. C. Jones, Aircraft measurements of water vapour continuum absorption at millimeter wavelengths, *Q. J. R. Meteorol. Soc.*, 120, 603–625, 1994.
- Eymard, L., L. Tabary, E. Gérard, S. A. Boukabara, and A. Le Cornec, The microwave radiometer aboard ERS-1, II, Validation of the geophysical products, *IEEE Trans. Geosci. Remote Sens.*, 34(C2), 291–303, 1996a.
- Eymard, L., et al., Study of the air-sea interactions at the mesoscale: The SEMAPHORE Experiment, *Ann. Geophys.*, 14, 986–1015, 1996b.
- Fung, A. K., and S. Tjuatja, Backscattering and emission signatures of randomly rough surfaces based on IEM, in *Proceedings of the International Geoscience and Remote Sensing Symposium*, pp. 1006–1008, Inst. of Electr. and Electron. Eng., New York, 1993.
- Gérard, E., and L. Eymard, Remote sensing of integrated cloud liquid water: Development of algorithms and quality control, *Radio Sci.*, this issue.
- Grant, E. H., S. Szwarnowski, and R. J. Sheppard, Dielectric properties of water in the microwave and infrared regions, *J. Am. Chem. Soc.*, 47 pp., 1981.
- Guillou, C., Etude du transfert radiatif dans l'atmosphère en micro-ondes à partir d'observations radiométriques aéroportées, Ph.D. thesis, 217 pp., Univ. of Paris-7, Paris, 1994.
- Guillou, C., S. J. English, C. Prigent, and D. C. Jones, Passive microwave airborne measurements of the sea surface response at 89 and 157 GHz, *J. Geophys. Res.*, 101(C2), 3775–3788, 1996.
- Guissard, A., and P. Sobieski, An approximate model for the microwave brightness temperature of the sea, *Int. J. Remote Sens.*, 8, 1607–1627, 1987.
- Hasted, J. B., D. M. Ritson, and C. H. Collie, Dielectric properties of aqueous ionic solutions, *J. Chem. Phys.*, 16, 1–11, 1948.
- Hasted, J. B., and S. H. M. El Sabeh, The dielectric properties of water in solutions, *Trans. Faraday Soc.*, 49, 1003–1011, 1953.
- Hewison, T. J., Reflectivity tests of microwave black body

- targets, *Met O (RSI), Branch Work. Pap.* 27, Met O (RSI), Hants, England, 1991.
- Ho, W. W., and W. F. Hall, Measurements of the dielectric properties of seawater and NaCl solutions at 2.65 GHz, *J. Geophys. Res.*, 78, 6301–6315, 1973.
- Ho, W. W., A. W. Love, and M. J. Van Melle, Measurements of the dielectric properties of sea water at 1.43 GHz, *NASA Contr. Rep. CR-2458*, 1974.
- Hollinger, J. P., DMSP special sensor microwave/imager: Calibration/validation, final report, vol. 2, Nav. Res. Lab., Washington, D. C., 1991.
- Jones, D. C., Microwave airborne radiometer and scanning system: Calibration and initial performance assessment, *Met O (RSI) Branch Memo.* 3, Natl. Meteorol. Library, Bracknell, England, 1991.
- Jones, D. C., S. J. English, R. W. Saunders, C. Prigent, C. Guillou, A. Chedin, and C. Claud, Aircraft microwave measurements at 89 and 157 GHz, *Proc. SPIE Int. Soc. Opt. Eng.*, 1935, 239–249, 1993.
- Klein, L. A., and C. T. Swift, An improved model for the dielectric constant of sea water at microwave frequencies, *IEEE Trans. Antennas Propag.*, AP-25, 104–111, 1977.
- Liebe, H. J., G. A. Hufford, and T. Manabe, A model for the complex permittivity of water at frequencies below 1 THz, *Int. J. Infrared Millimeter Waves*, 12, 659–675, 1991.
- Liebc, H. J., G. A. Hufford, and M. G. Cotton, Propagation modelling of moist air and suspended water/ice at frequencies below 1000 GHz, in *Proceedings of the AGARD 52nd Specialists' Meeting of the Electromagnetic Wave Propagation Panel*, pp. 3-1-3-10, Advis. Group for Aerosp. Res. and Dev., Brussels, Belgium, 1993.
- Monahan, E. C., and M. Lu, Acoustically relevant bubble assemblages and their dependence on meteorological parameters, *IEEE J. Oceanic Eng.*, 15, 340–349, 1990.
- Petty, G. W., and K. B. Katsaros, The response of the SSM/I to the marine environment, II, A parameterization of the effect of the sea surface slope distribution on emission and reflection, *J. Atmos. Oceanic Technol.*, 11, 617–628, 1994.
- Richards, M. G. M., and R. J. Sheppard, A precision waveguide system for the measurement of complex permittivity of lossy liquids and solid tissues in the frequency range 29 GHz to 90 GHz, II, The liquid system for 90 GHz; high-frequency cell design, *Meas. Sci. Technol.*, 2, 663–667, 1991.
- Rosenkranz, P. W., Rough-sea microwave emissivities measured with the SSM/I, *IEEE Trans. Geosci. Remote Sens.*, 30, 1081–1085, 1992.
- Ruf, C. S., S. J. Keihm, B. Subramanya, and M. A. Janssen, TOPEX/POSEIDON microwave radiometer performance and in-flight calibration, *J. Geophys. Res.*, 99(C12), 24,915–24,926, 1994.
- Sasaki, Y., I. Asanuma, K. Muneyama, G. Naito, and T. Suzuki, Microwave emission and reflection from the wind-roughened sea surface at 6.7 and 18.7 GHz, *IEEE Trans. Geosci. Remote Sens.*, 26, 860–868, 1988.
- Saxton, J. A., and J. A. Lane, Electrical properties of sea water, *Wireless Eng.*, 29, 269–275, 1952.
- Shutko, A. M., B. M. Liberman, and G. I. Chuhray, On the influence of dielectric property variations on the microwave radiation of a water surface, *IEEE J. Ocean. Eng.*, OE-7(1), 35–39, 1982.
- Stogryn, A., The apparent temperature of the sea at microwave frequencies, *IEEE Trans. Antennas Propag.*, AP-15, 278–286, 1967.
- Stogryn, A., Equations for calculating the dielectric constant of saline water, *IEEE Trans. Microwave Theory Tech.*, 19, 733–736, 1971.
- Ulaby, F. T., R. K. Moore, and A. K. Fung, *Microwave Remote Sensing*, vol. 3, Addison-Wesley, Reading, Mass., 1986.
- Wentz, F. J., A two-scale scattering model for foam-free sea microwave brightness temperatures, *J. Geophys. Res.*, 80, 3441–3446, 1975.
- Wentz, F. J., A model function for ocean microwave brightness temperatures, *J. Geophys. Res.*, 88, 1892–1908, 1983.
- Wilheit, T. T., A model for the microwave emissivity of the ocean's surface as a function of wind speed, *IEEE Trans. Geosci. Electron.*, GE-17, 244–249, 1979.
- Wisler, M. M., and J. P. Hollinger, Estimation of marine environmental parameters using microwave radiometric remote sensing systems, *NRL Memo. Rep.* 3661, Nov. 1977.
- Wu, S. T., and A. K. Fung, A noncoherent model for microwave emissions and backscattering from the sea surface, *J. Geophys. Res.*, 77, 5917–5929, 1972.
-
- G. Balana, G. Delbos, and W. Ellison, Laboratoire de Physique des Interactions Onde-Matière, ENSCPB, Université Bordeaux 1, 33402 Talence, France. (e-mail: balana@lmaster.u-bordeaux.fr; delbos@lmaster.u-bordeaux.fr; ellison@lmaster.u-bordeaux.fr).
- S. A. Boukabara, L. Eymard, and C. Guillou, Centre d'étude des Environnements Terrestre et Planétaires, Centre Universitaire, 10-12 avenue de l'Europe, 78140 Vélizy, France. (e-mail: sid-ahmed.boukabara@cetp.ipsl.fr; laurence.eymard@cetp.ipsl.fr; guillouc@cetp.ipsl.fr).
- K. Lamkaouchi, Département de Physique, Faculté des Sciences, BP4010, Meknès, Morocco. (e-mail: lamkaouchi@lmaster.u-bordeaux.fr).
- C. Prigent, Goddard Institute for Space Studies, 2880 Broadway, New York, NY 10025. (e-mail: kate@khamsin.giss.nasa.gov).

(Received February 18, 1997; revised September 3, 1997; accepted September 30, 1997.)